Kovove Mater. 50 2012 213–220
DOI: 10.4149/km_2012_4_213

Residual stress determination by neutron diffraction in a car gear-shaft made of 20NiCrMo2 alloyed case hardening steel

M. Rogante[1]*, M. Mazzanti[2], P. Mikula[3], M. Vrána[3]

[1]*Rogante Engineering Office, Contrada San Michele n. 61, 62012 Civitanova Marche, Italy*
[2]*Fiat Powertrain Technologies S.p.A., Corso Settembrini 167, 10135 Torino, Italy*
[3]*Nuclear Physics Institute ASCR, v.v.i., 25068 Řež, Czech Republic*

Received 25 August 2011, received in revised form 10 October 2011, accepted 16 December 2011

Abstract

The residual stresses (RS) induced in the substrate by case hardening treatment (HT) play a significant role in the behaviour of power train engineering components. In this paper, the results of RS investigation by neutron diffraction (ND) in 20NiCrMo2 steel car gear-shafts are presented. The RS were measured in correspondence of the critical region (notch) which is sensitive to fatigue-stress and/or crack, namely before/after a hardening treatment and after the successive finishing process. The achieved results can supply useful information on the effects of the various manufacturing processes on the RS status, better to evaluate the extent of distortion before and after the hardening treatment and to give a substantial support in the life assessment of the considered components. Furthermore, these results can yield parameters exploitable in monitoring of the hardening treatment characteristics, thereby confirming the relevance of thermal stresses induced by the same hardening treatment.

K e y w o r d s: 20NiCrMo2 steel, gear-shaft, case hardening, residual stress (RS), neutron diffraction (ND)

1. Introduction

Gear design is presently developing more and more and materials' choice is fundamental to optimize mechanical features with the aim to prolong the service life and downstream processing costs. Improved fatigue resistance (reducing failure phenomena brought about e.g. by bending and sub-surface fatigue and macro-pitting) can be directly associated with the design and manufacture control of materials, especially addition of alloying elements (Cr, Mn, Mo, Ni and others) to improve hardenability [1]. The ever-increasing performance and quality requirements call also for an enhanced quality of the heat treatment (HT) procedure, for instance by selecting complementary HTs with optimized process parameters.

Gear-shafts are normally submitted to the highest dynamic stresses in power train engineering. In order to obtain the specified strength properties [2], they are usually heat treated in atmospheric gas carburizing furnaces when using oil or nitrogen quenching. Just carburizing treatments are of major importance to develop fatigue and wear characteristics of steels. The relative case depth, which considers the components' size as well as the depth of carburized case, is one of the most important parameters determining fatigue performance [3]. New case hardening technologies, such as vacuum carburizing associated with high pressure gas quenching have been also developed in the recent years [4].

Case-hardenability (i.e., the material's ability to form more or less deep martensitic structure after hardening) is capable to give to the treated material adequate micro-structure and hardness in the high carbon surface. Performance life of carburized gear components usually depends on surface micro- and nano-structure, strength gradient, residual stress (RS), carbon content and steel cleanness [5]. The carburizing procedure can influence on the surface of the component grain size alteration and deformation. Moreover, local fluctuations of the chemical composition can promote dissimilar phase transformations in

*Corresponding author: tel.: +390733775248; fax: +390733775248; e-mail address: main@roganteengineering.it

the related vicinity, with consequent structure variations and inhomogeneous distortion. Hardenability can be considered in this context as an integrating parameter explaining the effect of the alloying elements and their distribution homogeneity in the structure on distortion [6]. Moreover, material properties after the HT process are influenced by various factors, which cannot be controlled by the HT process itself. Complex RS due to soft machining of the gears or inhomogeneities in the ingot material may produce negative treatment properties regarding microstructure and/or distortion [4, 7]. This can lead to low process-capability factors regardless of a high quality HT. Therefore, it is important to know the RS status, mainly in correspondence of key zones of the gear-shaft which are predominantly sensitive to fatigue stress and/or crack. RS, together with hardness distribution, micro- and nano-structure, surface finish and geometry, represent the main factors that influence fatigue strength. Compressive RS usually resist those applied (generally tensile) that cause fatigue failure [1]. Since the RS distribution affecting the fatigue cracks nucleation is a key factor able to control the gear performance, it is clear that the RS-gradients should be accurately determined.

Some RS assessments related to case hardening steels via conventional methods including hole drilling and X-ray diffraction (XRD) have been carried out in the past. Compact specimens made of 20NiCrMo2 steel were analysed, e.g., by using the incremental hole-drilling method, in order to investigate the effects of the RS field resulting from shot peening and the indentation technique in relation to fatigue crack closure and crack growth behaviour [8]. The characterization of RS in gas carburized SAE 8620 steel samples was carried out, e.g., using XRD and the bending fatigue performance was evaluated comparing high temperature gas carburized steel with conventional temperature gas carburization. The results showed that the fatigue performance of the high temperature gas carburized specimens was rather poor compared to the typically gas carburized specimens [9].

Neutron methods have recently become an increasingly significant probe for materials across a wide range of disciplines and among other ones they are becoming more and more helpful in the characterization of materials and components of industrial interest, revealing significant properties related to the investigated objects [10–13]. Their peculiarity, with respect to other investigation techniques, is the possibility of giving full information about the micro- and nano-physical structure of the material sub-surface in a non-destructive way. In the case of RS measurements the main advantage of ND over other methods is that they can provide required information in the range of the depth from several tenths of millimetres up to several centimetres. As the XRD technique, in fact, according to the atomic number of the investigated material allows measuring surface RS only to a depth of several tens of micrometres both non-destructive diffraction methods can supplement each other when permitting RS investigations from the extreme surface to deep without any layer removal or hole drilling [14].

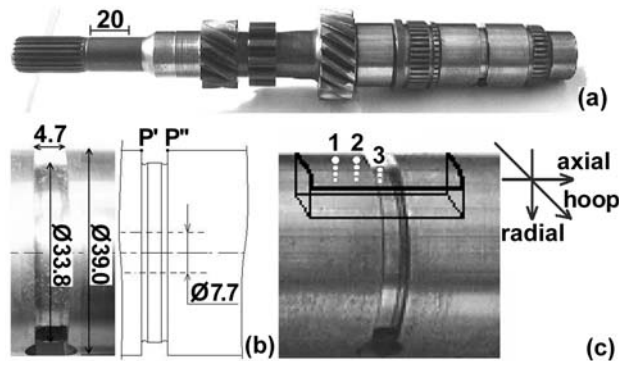

Fig. 1. The 20NiCrMo2 steel car gear-shaft investigated by neutron diffraction (a), a detail (b) and the geometry of measurements (c).

In the present experiment ND was used for determination of RS level in the chosen part of a car gear-shaft made of 20NiCrMo2 alloyed case hardening steel.

2. Materials and methods

2.1. Samples description

Figure 1 shows the gear-shaft investigated and the measurement details. The constitutive material is a 20NiCrMo2 steel (reference standard: UNI 7846; comparable standards: AISI/SAE 8620; AFNOR 20NCD2; SIAU HD20). This is a structural steel with carbon content less than 0.30 % intended for HT, consisting in carbon enrichment of the part surface and subsequent hardening to obtain high level surface hardness, with excellent wear strength while the low carbon content of the core promotes high level toughness of the underlying mass. Case hardening steels are generally used to fabricate mechanical parts, such as gears of any type, axles, cones, pinions, king pins, bushes, ratchets, lead nuts, distribution and drive shafts. A further use concerns high tensile applications in the non-carburized status, but through hardened and tempered. The 20NiCrMo2 grade is suitable for small and medium parts of intricate shape, for which oil quenching and low level distortion after treatment are required. The chemical composition is shown in Table 1, while typical mechanical properties, with reference to the material (as quenched and tempered at 200 ℃) and to the sections in the range 25–100 mm, are the following: yield strength: 690–493 MPa; tensile

Table 1. Chemical composition of the 20NiCrMo2 steel

Element	C	Si	Mn	S	P	Cr	Ni	Mo	Fe
min.	0.17	0.15	0.60			0.35	0.40	0.15	bal.
max.	0.23	0.40	0.90	0.035	0.035	0.65	0.70	0.25	

strength: 925–740 MPa; elongation: 17–20 %; hardness: 275–220 HB.

The manufacturing procedure of this gear-shaft is carried out through the following consecutive steps: cut and extrusion of the original forged billet to obtain a bar; isothermal annealing ($\sim 950\,^{\circ}$C); machining by chip removal; HT (~ 8 h in atmospheric gas carburizing furnaces at $\sim 900\,^{\circ}$C, using hot oil quenching at $\sim 120\,^{\circ}$C; thickness ~ 0.7 mm); straightening process made by using a $\sim$ 20 ton electromechanical press; external contour grinding (finishing). The main aims of the adopted HT are: to create adequate strength gradients to withstand the stress gradients and supply a satisfactory safety level; to produce a fine martensitic microstructure; to increase hardness according to penetration of the martensitic transformation in the part section; to eliminate as more as possible surface wear. The aim of the straightening process is to eliminate the buckling of the shaft axis produced by the HT.

2.2. Neutron diffraction for residual stress measurements

It is clear that in the case of ND measurements on polycrystalline samples, neutrons are sensitive to the crystalline structure and its changes. RS are not measured directly but they are determined from measurement of residual strains, which are then converted to stresses using appropriate moduli. The neutrons from the sample gauge volume are diffracted by a family of lattice planes (hkl) under the $2\theta_{hkl}$ scattering angle, according to the Bragg law:

$$2d_{hkl}\sin\theta_{hkl} = \lambda, \tag{1}$$

where d_{hkl} is the measured interplanar spacing, θ_{hkl} is the Bragg angle – i.e., one-half the scattering angle for a diffraction peak corresponding to the crystallographic Miller indices (h, k, l) – and λ is the neutron wavelength.

The differentiated Bragg equation gives a relative lattice strain ε_{hkl} in the form:

$$\varepsilon_{hkl} = \frac{d_{hkl} - d_{0,hkl}}{d_{0,hkl}} = \frac{\Delta d_{hkl}}{d_{0,hkl}} = -\cot\theta_{hkl}\Delta\theta_{hkl}, \tag{2}$$

where $d_{0,hkl}$ is the stress-free interplanar spacing.

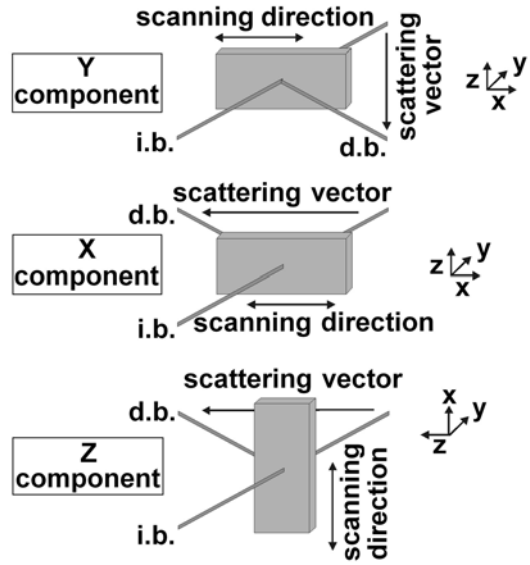

Fig. 2. Scheme of the experimental sample arrangement usually used for the through-the-thickness strain component scanning (i.b. – incident beam; d.b. – diffracted beam).

The strain determination is based on measurements of angular deviation $\Delta\theta_{hkl}$ of the diffraction profile position from the value related to the stress-free state. The analysis of tri-axial stress states, in particular, requires accurate values of the unstressed interplanar spacing. A strain free sample of the material avoids systematic errors in the $d_{0,hkl}$ – and hence in the strain value – and various experimental and analytical methods exist for the determination of $d_{0,hkl}$, which are discussed in [15].

The σ_x stress component can be obtained, consequently, by knowing the diffraction elastic Young's modulus E_{hkl} and the diffraction Poisson's ratio ν_{hkl} of the considered material and using the Hooke's law in the form:

$$\sigma_x = \frac{E_{hkl}}{(1-2\nu_{hkl})(1+\nu_{hkl})} \cdot \cdot \left[(1-\nu_{hkl})\varepsilon_x^{hkl} + \nu_{hkl}(\varepsilon_y^{hkl} + \varepsilon_z^{hkl})\right], \tag{3}$$

where $\varepsilon_{x,y,z}^{hkl}$ is the x, y, z-component of the lattice strain measured on the crystal lattice planes (hkl). The $\varepsilon_{x,y,z}^{hkl}$ lattice strain components are determined in the ND experiment. Corresponding relations for other y and z stress components are obtained by simple permutations of x, y and z indexes. A through-the-thickness mapping of residual strains was then carried out with reference to the experimental arrangement shown in Fig. 2. The sample gauge volume was defined by using two fixed slits in the incident and diffracted beam, respectively. The specimen was moved step by step in the z direction and the corresponding

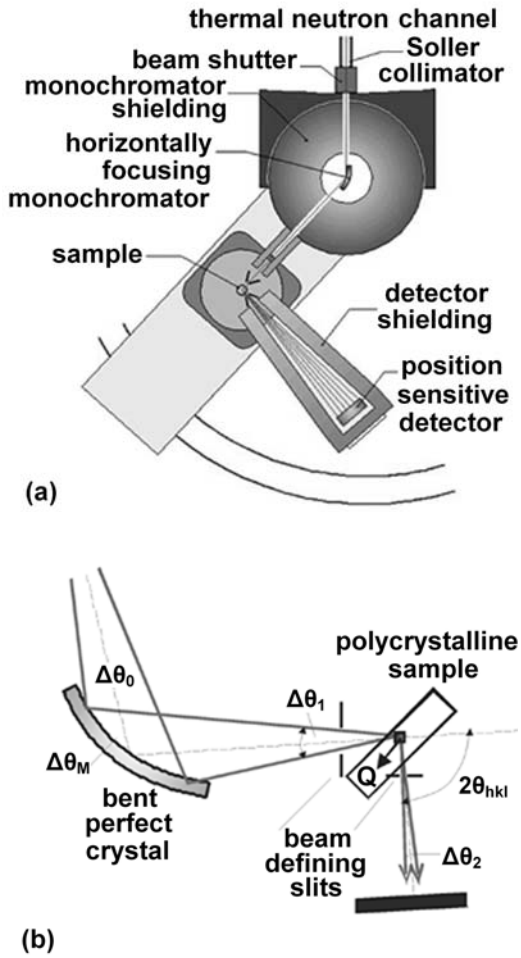

Fig. 3. Schematic layout of the double axis diffractometer adopted for the stress investigation (a) and the detailed geometry of the diffractometer focusing performance (b). $\boldsymbol{Q}$ is the scattering vector perpendicular to the diffraction lattice planes.

diffraction spectra are collected in each position. The corresponding component of the strain tensor is adjusted by a proper rotation of the specimen with respect to the scattering vector $\boldsymbol{Q}$.

3. Experimental procedures and results

The measurements were carried out on the neutron diffractometer adapted for strain scanning, which is installed at the medium power reactor LVR-15 in Řež (Fig. 3). This dedicated diffractometer is particularly suitable for macro/micro strain scanning of polycrystalline materials. It uses advantages coming from focusing both in real and momentum space and yields good resolution and luminosity, especially for samples of small dimensions. The resolution properties of the device are reached in a limited Q-range for which the focusing conditions are optimized. In the strain scanning by this instrument, the gauge volume is determined by two fixed Cd slits – (2–5) × (3–30) mm^2 – in the incident, and diffracted beams and the measurements are usually performed in the vicinity of the scattering angle $2\theta_{hkl} = 90°$. For these values of $2\theta_{hkl}$ the typical uncertainty in determining the strain is slightly less than 10^{-4}. In our case the neutron wavelength of $\lambda = 2.35$ Å was used, which for Fe(110) reflection determines the scattering angle $2\theta_{110} = 70°$. The following elastic and Poisson's constants were employed: $E = 225.5$ GPa; $\nu = 0.28$. Different sample spatial positions were investigated by using a gauge volume of $1 \times 1 \times 2$ mm^3. In all cases $d_{0,hkl}$ necessary for strain evaluation was determined by measurement on small coupons cut in different depths from the surface.

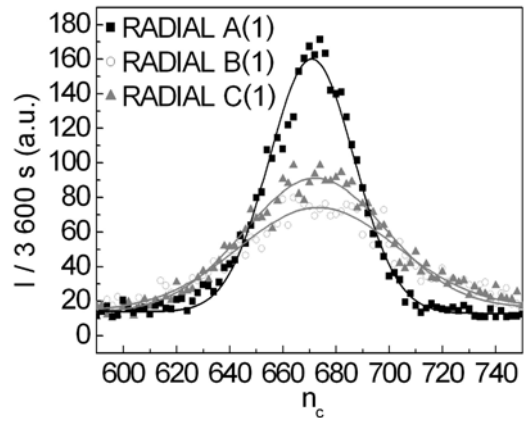

Fig. 4. Diffraction profiles (intensity of diffracted neutrons vs. diffraction angle 2θ determined by a channel number of the position sensitive detector) related to the measurements carried out on the cut samples before the HT (A), after the HT (B) and after the finishing process (C).

In the stress investigations, two procedures were used. In the first case three gear-shafts (as whole) were examined. In the second case samples obtained by sectioning of these shafts in correspondence to the critical zones were investigated (Fig. 1c). With reference to Fig. 1c, line 3 corresponds to the centre of the notch, line 2 is 5 mm distant from line 3 and analogously line 1 from line 2 before/after HT and after the successive finishing process. In the course of all measurements one important phenomenon appeared. HT affected the originally ferrite crystallographic structure, which was then partly transformed in the martensite structure. It can be seen from Fig. 4, which shows diffraction profiles (intensity of diffracted neutrons vs. diffraction angle 2θ determined by a channel number of the position sensitive detector), related to the measurements carried out in the cut sample before the HT (A), after the HT (B) and after the finishing process (C) in correspondence of the line 1 (Fig. 1) at 5 mm of depth from the surface, with reference to the radial direction.

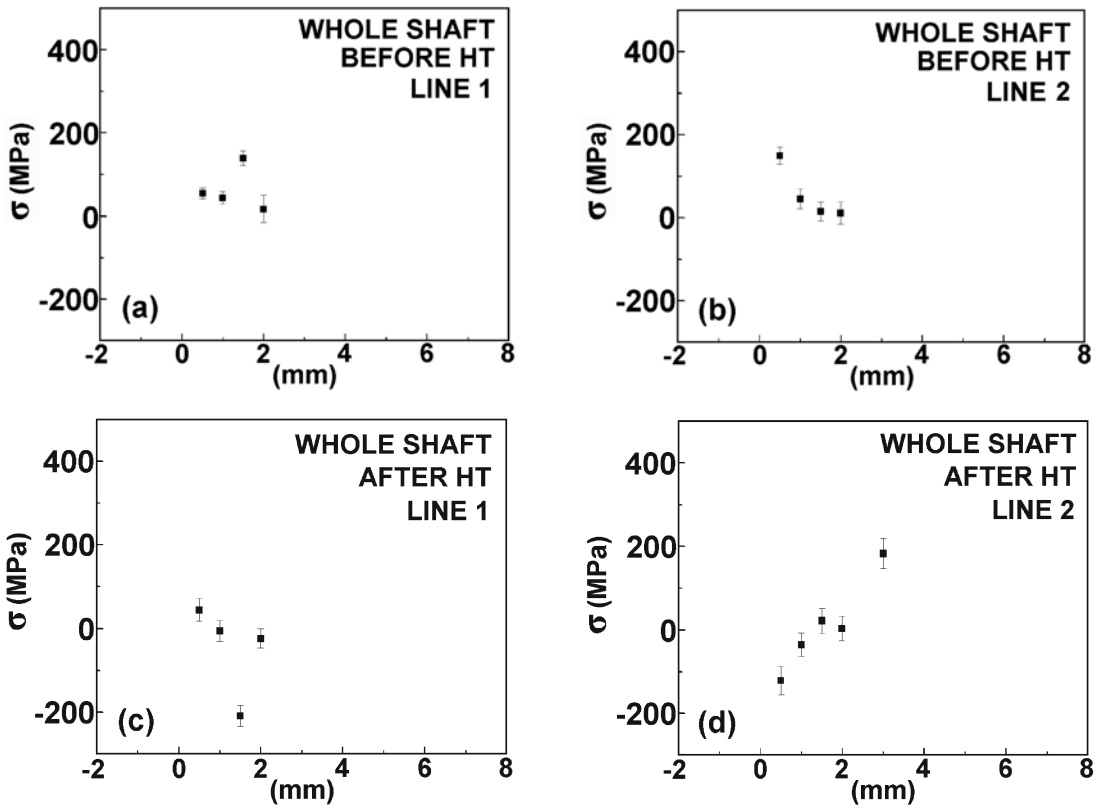

Fig. 5. RS hoop component determined in correspondence of line 1 and 2 (whole gear-shaft), as differences between the RS status before an after the case-hardening treatment.

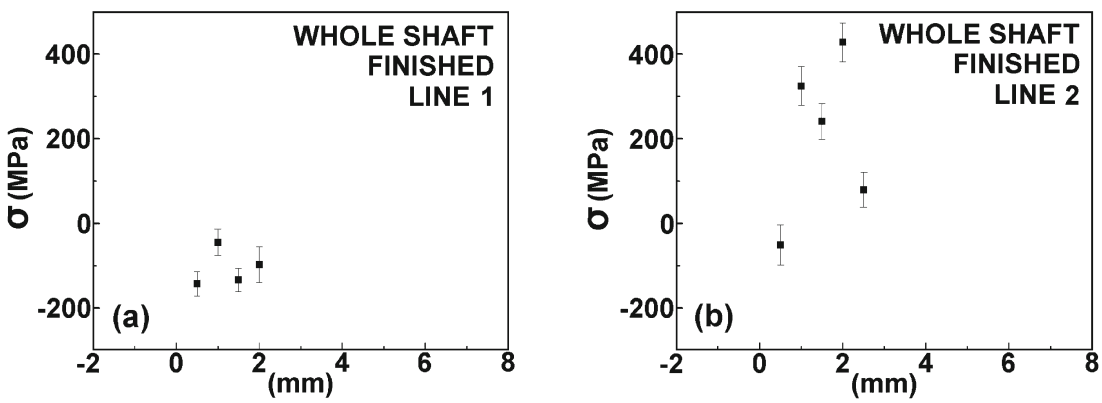

Fig. 6. RS hoop component determined in correspondence to lines 1 (a) and 2 (b) (whole gear-shaft), as differences between the RS status after the finishing process and before the case-hardening treatment.

In the case of the investigations related to the whole samples, two cycles of measurements were carried out – one in the transmission (ε_x), corresponding to the hoop direction, the other in the reflection (ε_z) configuration. In each cycle, the lines shown in Fig. 1 were scanned. The specimen was moved step by step in the z (radial) direction and the corresponding diffraction spectra were collected in each position. The corresponding component of the strain tensor was adjusted by a proper rotation of the specimen with respect to the scattering vector. The macroscopic stress component σ_x parallel to the sample surface (i.e., the hoop component) was calculated by subtracting σ_z. As σ_z was considered very small, the following simplified form resulted for σ_x:

$$\sigma_x \approx \sigma_x - \sigma_z = \frac{E}{(1+\nu)}(\varepsilon_x - \varepsilon_z). \qquad (4)$$

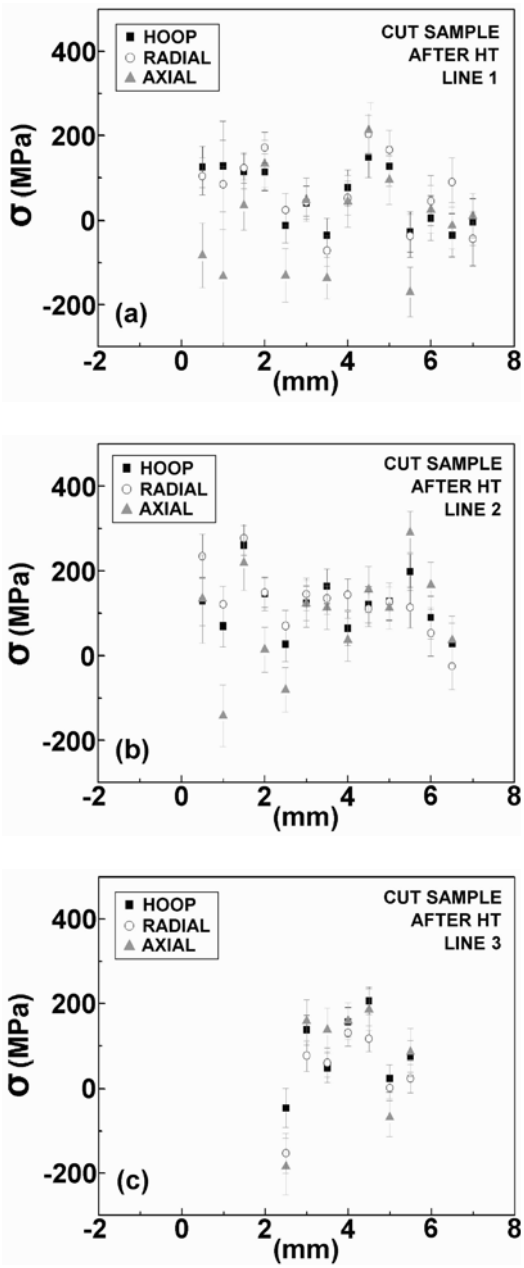

Fig. 7. RS components determined in correspondence of line 1 (a), line 2 (b) and line 3 (c) after the case-hardening treatment (cut sample).

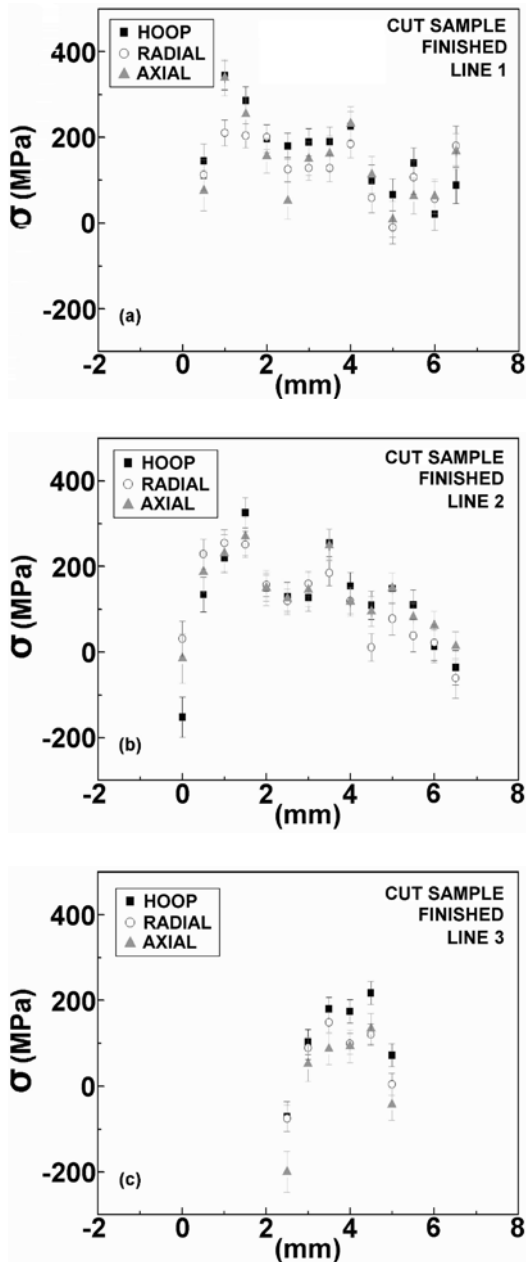

Fig. 8. RS components determined in correspondence of line 1 (a), line 2 (b) and line 3 (c), as differences between the RS status after the finishing process and before the case-hardening treatment (cut sample).

In this case, no standard sample was necessary. By using this procedure, we received stress results shown in Figs. 5 and 6. With reference to Fig. 1c and to the whole gear-shafts, Fig. 5 shows the RS hoop components determined in correspondence of lines 1 and 2, respectively, as differences between the RS status before and after the HT procedure. Figure 6 shows differences between the RS status after the finishing process and before the HT. It should be pointed out that this procedure was used (and can be used) as a way of determination of RS status on the samples of rather complicated forms. Therefore, for the whole gear-shaft, in reason of its geometry in the zone interested by the analysis, the RS hoop component only was determined.

On the other hand, through-the-thickness residual strain measurements along the three main directions (hoop, radial and axial) could be performed for the cut samples obtained by sectioning of the considered shafts in correspondence of the mentioned critical zone. One of the goals of the measurements was to find out the RS status in the sample after HT and

after the finishing the process in relation to the status before HT. Therefore, the status before HT served as an initial standard providing the necessary parameters for evaluation of the RS status after HT and after the finishing the process which are shown in Figs. 7 and 8.

4. Discussion

The RS related to the shaft (or its section) before the HT, as mentioned, were considered nearly homogeneous. To highlight much more the effects of the HT, the strain status before HT was taken as a reference to determine RS after the HT and after the successive finishing process: these RS were calculated, in fact, employing the difference between the strain conditions preceding and successive HT. RS shown for the shaft or its sections after HT represent, in fact, their real values due to the effects of the same HT. RS are mainly due to the HT and secondarily to the thermal mismatch and temperature gradients effects. Thus, with reference to Fig. 1b, it should be underlined that in the points P' and P" RS axial and radial components are considered to be zero, but this is not valid in the other zones, including those adjacent. So, existing RS gradients are also responsible for the measured differences between lines 1 and 2 (Fig. 1c). At the surface, besides, the radial RS component is always zero. Inspection of Fig. 5c (after HT, line 1) reveals that the hoop RS component starts from values close to zero in correspondence to the first superficial layer of 1 mm, then becomes compressive reaching about –200 MPa and then returns again to value close to zero. On the other hand for line 2 (Fig. 5d) the hoop RS start from about –100 MPa in correspondence to the first superficial layer of 1 mm, then pass to a tensile status ($\sim$ 200 MPa) at the depth of about 3 mm. As can be seen from Fig. 6a, which refers to line 1, after finishing the process, the hoop RS values alternate in the vicinity of the value of –100 MPa. However, hoop components of the RS related to line 2 (i.e., in proximity of the diameter variation), starting from values close to the zero in correspondence of the first superficial layer of 1 mm, increase up to $\sim$ 400 MPa at the depth of 2 mm (Fig. 6b).

Figures 7 and 8 show the RS status in the cut samples after HT as well as after finishing the process (before HT). In the case of results presented in Figs. 7c and 8c, the measurements started from the value of 2.5 mm (abscissa), corresponding to the outside surface of the notch. The radial component has values next to the zero, while the other two components, starting from slight tensile values in correspondence of the first superficial layer of 1 mm, move to slight compressive values in higher depth. In reference to Figs. 7a or 7b, there is a similar behaviour of the radial and hoop components alternating between –100 MPa and 200 MPa or zero and 200 MPa, respectively. However, there is not smooth behaviour of the axial component, which alternates between –200 MPa and 200 MPa. Similarly, the RS components related to line 3 (Fig. 7c) alternate in the range –200 MPa and 200 MPa and the hoop component alternates between values next to the zero and a tensile status of $\sim$ 200 MPa. In the case of the cut sample after the finishing process (Fig. 8), the RS component behaviours related to lines 1 and 2 appear similar, but with a greater affinity between the three RS components. The hoop component reaches the most extreme values (from almost zero to $\sim$ 350 MPa).

Inspection of Figs. 7 and 8 reveals that the experimental errors of the obtained results are rather larger than in the case of the results related to the samples before the HT. It follows from the fact that the RS components obtained after the HT or after the finishing process were related to the RS components corresponding to the status before HT. Moreover, after HT, the diffraction profiles became wider with much smaller peak profiler intensity (as shown in Fig. 4), due to the presence of the martensitic phase.

5. Conclusions

The measurement feasibility and the industrial applicability of ND technique in the power train engineering sector have been shown. The data obtained are easily interpretable and supply indications that can be considered as a reference in determining strains and RS in gear-shafts and other mechanical components of the same constitutive material as that analysed or made with similar materials. Measurement can be carried out starting from the surface and the subsurface until 5–6 mm of depth, in different situations. The achieved results are useful as: information to the knowledge of the involved material, contributing to evaluate its characteristics and behaviour; indications on the effects of HT and in the monitoring of its characteristics when supplying a substantial support in the life assessment of the component; contribution to the enhancement of FEM calculations. These results can be exploited to optimize the operative conditions and/or modify the HT parameters, with the aim of achieving the most appropriate RS gradients and thus in the perspective of developing advanced gear box technologies such dual clutch or 6-speed automatic gearboxes. A complementary micro- and nano-structural characterization by small-angle neutron scattering, finally, would allow monitoring key parameters such as size and concentration of inhomogeneities (micro- and nano-defects such as precipitates-carbides and voids), their volume fraction and an interface area. The mentioned parameters can

superimpose with the RS status and can make worse the risk of cracks during the straightening of the shaft; knowledge of these parameters can help the manufacturer in assessing the origin of the present RS, enhancing the quality of HT procedure and supporting the life assessment of the component. Finally, it can be stated that the applicability of ND technique to engineering science offers significant information not available by any other method. The near future can offer substantial opportunity for new improvements in the optimization of neutron instruments, techniques and data treatments related to the strain scanning of industrial materials.

Acknowledgements

This work has been supported by a grant project of GACR P204/12/1360 and EC under the FP6 through the Key Action: Strengthening the European Research Area, Research Infrastructures, Contract n° R113-CT-2003-505925, and FP6-NMI3 Programme – ACCESS to Large Scale Facilities.

References

[1] Herring, D. H.: Gear Techn., *3/4*, 2004, p. 35.
[2] Löser, K.: In: Proceedings Int. Conf. Steels in Cars and Trucks 2005. Eds.: Hagen von, I., Wieland, H. J. Düsseldorf, Verlag Stahleisen GmbH 2005, p. 237.
[3] Genel, K., Demirkol, M.: Int. J. Fatigue, *21*, 1999, p. 207. doi:10.1016/S0142-1123(98)00061-9
[4] Löser, K.: In: Proceedings 9th Int. Trade Fair and Symposium for Thermo Process Technology. Frankfurt am Main, VDMA Thermo Process Technology Association 2007, p. 1.
[5] Krauss, G.: Heat Treating, *4*, 1993, p. 12.
[6] Prinz, C., Clausen, B., Hoffmann, F., Kohlmann, R., Zoch, H. W.: Materialwissenschaft und Werkstofftechnik, *37*, 2006, p. 29. doi:10.1002/mawe.200500949
[7] Cristinacce, M.: In: Proceedings 18th Conference Heat Treating. Eds.: Wallis, R. A., Walton, H. W. Materials Park, USA, ASM International 1998, p. 5.
[8] Farrahi, G. H., Majzoobi, G. H., Hosseinzadeh, F., Harati, S. M.: Eng. Fract. Mech., *73*, 2006, p. 1772. doi:10.1016/j.engfracmech.2006.03.004
[9] Asi, O., Can, A. Ç., Pineault, J., Belassel, M.: Mater. Des., *30*, 2009, p. 1792. doi:10.1016/j.matdes.2008.07.020
[10] Rogante, M.: In: Proceedings 1st Italian Workshop for Industry Applicazioni Industriali delle Tecniche Neutroniche®. Ed.: Rogante, M. Civitanova Marche, Italy, Rogante Engineering 2008, p. 40.
[11] Rogante, M., Rosta, L.: In: Proceedings of SPIE 5824, Opto-Ireland 2005: Nanotechnology and Nanophotonics. Eds.: Blau, W. J., Kennedy, D., Colreavy, J. Bellingham, WA, SPIE 2005, p. 294.
[12] Rogante, M.: Oil Gas J., *103*, 2005, p. 59.
[13] Rogante, M.: In: Proceedings MATRIB '03. Ed.: Grilec, K. Zagreb, Croatian Society for Materials and Tribology 2003, p. 235.
[14] Rogante, M., Mikula, P., Vrána, M.: Key Eng. Mat., *465*, 2011, p. 259. doi:10.4028/www.scientific.net/KEM.465.259
[15] Rogante, M.: Phys. B, *276–278*, 2000, p. 202. doi:10.1016/S0921-4526(99)01281-8